



Provided by the author(s) and University of Galway in accordance with publisher policies. Please cite the published version when available.

Title	A computational toolchain for the automatic generation of multiple Reduced-Order Models from CFD simulations
Author(s)	Marzullo, Thibault; Keane, Marcus M.; Geron, Marco; Monaghan, Rory F. D.
Publication Date	2019-05-25
Publication Information	Marzullo, Thibault, Keane, Marcus M., Geron, Marco, & Monaghan, Rory F. D. (2019). A computational toolchain for the automatic generation of multiple Reduced-Order Models from CFD simulations. <i>Energy</i> , 180, 511-519. doi: https://doi.org/10.1016/j.energy.2019.05.094
Publisher	Elsevier
Link to publisher's version	https://doi.org/10.1016/j.energy.2019.05.094
Item record	http://hdl.handle.net/10379/17346
DOI	http://dx.doi.org/10.1016/j.energy.2019.05.094

Downloaded 2024-04-29T08:54:14Z

Some rights reserved. For more information, please see the item record link above.





A computational toolchain for the automatic generation of multiple Reduced-Order Models from CFD simulations

Thibault Marzullo ^{a, b, c, *}, Marcus M. Keane ^{a, b, c}, Marco Geron ^d, Rory F.D. Monaghan ^{a, b, c}

^a School of Engineering, National University of Ireland Galway, Galway, Ireland

^b Ryan Institute, Galway, Ireland

^c Research Centre for Marine and Renewable Energy, Galway, Ireland

^d School of Mechanical and Aerospace Engineering, Queen's University Belfast, Belfast, United Kingdom

ARTICLE INFO

Article history:

Received 28 November 2018

Received in revised form

5 April 2019

Accepted 13 May 2019

Available online 18 May 2019

Keywords:

CFD

ROM

Buildings

Zonal model

ABSTRACT

This paper describes the development of a systematic tool chain capable of automatically extracting accurate and efficient Reduced-Order Models (ROMs) from Computational Fluid Dynamics (CFD) simulations. These ROMs can then be used to support the design and operation of Near-Zero Energy Buildings (NZEB), with a higher accuracy than traditional zonal models but at a fraction of the computational cost of CFD. This study assesses the accuracy and time to solution of these ROMs when solved for appropriate Boundary Conditions (BCs), found in the built environment, in order to define the usability envelope of the automatically extracted ROMs. The parameters used in this study are inlet temperatures (K) and mass flow rates (kg/s). Results demonstrate that the absolute error can be maintained at under 0.5 K for changes in temperature of up to ± 15 K, and under 0.25 K for changes in mass flow rates of up to $\pm 45\%$ of the original value. The results show that this method has the potential for applications in the built environment where the ROM accuracy and low computational cost can bridge a gap between low order RC models and high order CFD, further improving the energy efficiency in smart buildings.

Crown Copyright © 2019 Published by Elsevier Ltd. All rights reserved.

1. Introduction

In the recent and ever growing global motivation for the development of the sustainable production and usage of energy, buildings are being adapted with varying degrees of “smartness”. Construction materials, urban planning, architecture and systems management are being carefully optimized, as designers develop or retrofit an increasing number of buildings to render them Near Zero Energy Buildings (NZEB) in accordance with the EU Energy Performance Building Directive 2010/31/EU. With the advent of modern computing it is common to simulate parts or the entirety of a building in order to make informed design choices. In addition, smart buildings can benefit from the information gathered and processed by Building Energy Management Systems (BEMS) during their operational phase.

These systems rely not only on the accuracy of the data gathered through sensors, but also on the accuracy of computer models needed to predict a response to a certain change in energy inputs. Ideally, these models should be extremely accurate. In reality, the computational requirements of such models can become so important as to render them completely impractical. Models are therefore simplified and guided by required accuracy of the results in the intended target application domain.

1.1. Models used in building energy simulations

When rapid solutions are needed, domains are usually simplified as nodal models. Such models assume that entire portions of a building can be approximated by a single uniform space, or a node. This allows designers to evaluate energy consumption by running a large number of simulations, which is the case when yearly consumption estimates are needed or when the building stock of entire districts for load forecasting [1] or demand side management [2], but also towns [3] must be simulated. A review from Allegrini et al. (2015) [4] focuses on district level modelling. Nodal models can be expanded to become multi-nodal models, which allow estimation of energy exchanges within a building and provide a better

* Corresponding author. School of Engineering, National University of Ireland Galway, Galway, Ireland.

E-mail addresses: t.marzullo1@nuigalway.ie (T. Marzullo), marcus.keane@nuigalway.ie (M.M. Keane), m.geron@qub.ac.uk (M. Geron), rory.monaghan@nuigalway.ie (R.F.D. Monaghan).

Abbreviations

BC	Boundary Condition
BEMS	Building Energy Management System
CFD	Computational Fluid Dynamics
CFD-ROM	Computational Fluid Dynamics – Reduced Order Model
MultiCFD	ROM extracted and solved for the same BCs
MultiROM	ROM extracted and solved for different BCs
NZEB	Near Zero Energy Buildings
RANS	Reynolds Average Navier-Stokes
RNG	Re-Normalisation Group
ROM	Reduced Order Model
WMAE	Weighted Mean Absolute Error (in K)

representation of energy consumptions. These models are often based on electrical circuit analogy such as presented in Refs. [5,6] and are used for example for estimating energy consumption [7] or thermal comfort [8] in buildings.

For a more accurate description of thermal exchanges within a room or a building, zonal models are used. They subdivide a zone such as a room into several subzones and can be used to simulate effects such as thermal stratification, air plumes above convectors or air jets at HVAC inlets [9]. This type of approach is also useful when studying user thermal comfort, air mixing and indoor air quality, all of which can vary greatly within a single room. Megri et al. [9] published a review on zonal models and their applications. Zonal models usually rely on user expertise for the definition of each subzone. The number of sub-zones, their location in the domain and the properties of each are defined manually by the modeller, making it a time-consuming and error-prone process.

1.2. CFD applications in the built environment

For studying flow patterns more closely, designers have access to Computational Fluid Dynamics (CFD) modelling technologies. The CFD modelling technique subdivides a numerical domain into many smaller finite volumes, usually hundreds of thousands to millions of computational cells. By computing partial differential Navier-Stokes, mass and energy balance equations between each cell and over the entire numerical domain, CFD simulations can provide an accurate description of flow magnitude and direction, thermal exchanges, distributions of temperature, pressure, density, and other properties.

The main drawbacks of CFD are high computational cost and the extensive user expertise needed to accurately model the boundary conditions, which have an important impact on the final results.

CFD simulations are used to assess indoor air quality and pollutant dispersion [10], thermal comfort [11], and are extensively used in studies relating to naturally ventilated buildings such as in Ref. [12]. Etheridge (2015) presents CFD as a suitable method in a review on natural ventilation [13]. CFD is also often used when simulating urban environments, in which researchers studied the effects of urban heat islands [14], wind profiles in streets [15] and around buildings [16]. Like for indoor environments, CFD is used for studies on outdoor pollutant dispersion [17]. The impact of wind canyons and densely built environments on city breathability has been simulated with CFD in Ref. [18], and likewise the impact of vegetation as seen in Ref. [19].

1.3. CFD model order reduction

In an effort to leverage CFD's accuracy at a fraction of the computational cost, researchers have developed techniques aimed at simplifying or extracting reduced order models (ROMs) from CFD simulations. The literature presents methods such as the Pressure Implicit with Splitting of Operator (PISO) method [20] which is derived from the Semi-Implicit Method for Pressure-Linked Equations (SIMPLE) algorithm [21] and have been developed for non-iterative computation of unsteady flows and later extended to steady-state, but it has important computational costs. This can be mitigated by using semi-Lagrangian PISO [22] which has a lower computational cost than PISO. Proper Orthonormal Decomposition (POD) [23] and balanced POD [24], are used to reduce a model's number of degrees of freedom when information on the flow pattern must be captured. Fast Fluid Dynamics (FFD) [25] is derived from projection methods [26] and allows real-time solution of Navier-Stokes equations and is typically applied to wind load calculations.

Generally, the development of these models is heavily dependent on the modeller's level of expertise. Each reduced order model is developed or requires adaptation to fit a specific domain problem, and therefore requires the input of an expert. It would be beneficial to have access to a systematic automated approach to facilitate model order reduction. This study proposes a method to leverage the results from an existing CFD simulation to automatically generate rapid and accurate zonal models without additional user expertise. These zonal models can then be used to simulate conditions for which no CFD simulation is available while retaining a high level of accuracy within a proposed domain.

2. Methodology

The proposed method for ROM generation automatically extracts a multi zonal model from a CFD simulation, which can then be solved for boundary condition parameters different from the original CFD. The main advantages of this method are the level of automation, which allows generation of ROMs with minimal user input and expertise; the level of fidelity compared to CFD, which enables the ROM to retain most of the CFD simulation's accuracy; and finally the computational cost, which allows the generation of ROMs in under 60 s and their solution in under 0.95 s.

The CFD-ROM method consists in 6 main steps as shown in Fig. 1: (1) the results of a CFD simulation are imported, (2) CFD computational cells are clustered together to create zones, which are uniform volumes of air, (3) interactions between zones and between zones and domain boundaries are processed, (4) a ROM is generated and (5) solved, and finally (6) the solved ROM is remapped back to the CFD domain.

This section presents the methods used in the development of the algorithms in Python [27] for extraction and solution of the ROMs. Firstly, it presents the CFD simulations on which the ROMs have been tested and assessed, then the principles of zone generation, ROM generation and solution are explained.

2.1. CFD simulations and validation

The data used in this comparative study are taken from the previously-validated CFD model of a north-facing office in the Environmental Research Institute (ERI) building at University College Cork (UCC), shown in Fig. 2 [28]. The office measures 5.2 m (length) by 5.6 m (width) by 2.9 (height). Its furniture includes five

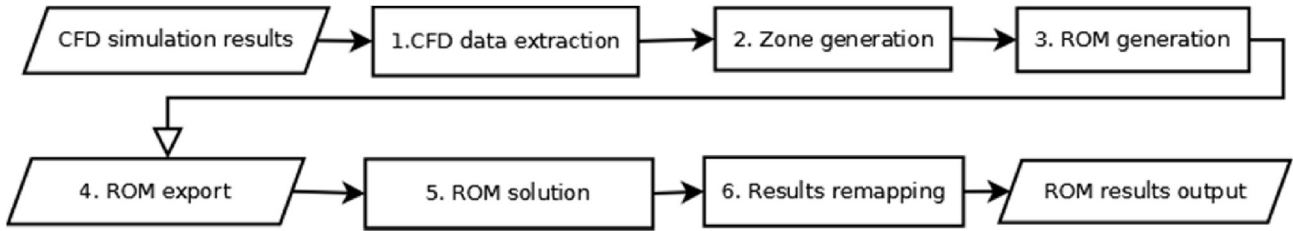


Fig. 1. CFD-ROM method flowchart outlining the main steps of the method.

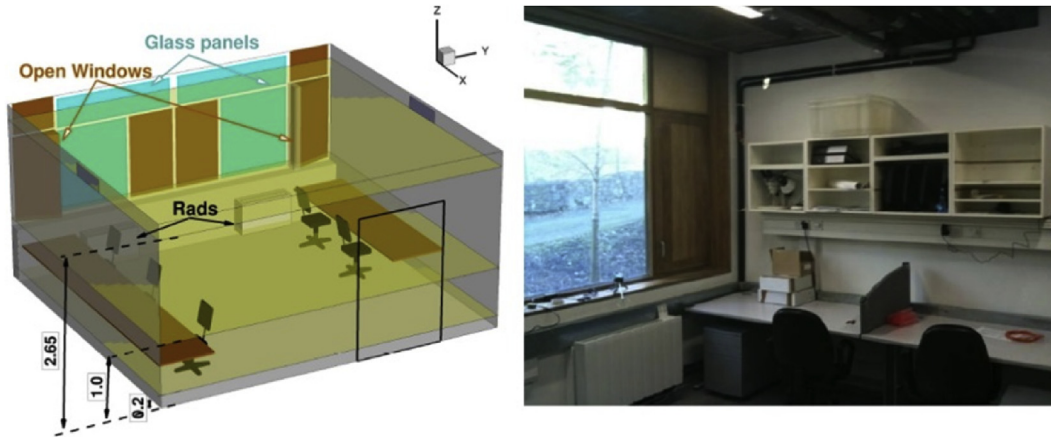


Fig. 2. Numerical and physical domain of the ERI building office modelled in CFD.

desks and chairs and shelf units. Two fan convectors heat the office and two automated windows are present. No other sources of heating, such as computers or people, are present. Steady state CFD models were developed using the Phoenics modelling software [29], which uses an immersed body technique. Therefore, a Cartesian structured grid was defined with 1,572,165 cells (115 × 147 × 93). Turbulence was modelled using the Reynolds Average Navier-Stokes (RANS) approach coupled with the Re-Normalisation Group (RNG) *k-ε* turbulence model. Air was modelled as an incompressible ideal gas. The ceiling, floor, east and

west walls were assumed to have a constant temperature. All other objects are considered adiabatic. All CFD simulations used have been validated with experimental data and previously published [28].

The CFD domain energy sources are listed in Table 1. In the case used for this study, the windows and door are closed and the two convectors are in an on state. The domain includes two air vents located on the east and west walls close to the ceiling. The two convectors are located on the north wall, close to the windows.

Table 1
CFD simulation base boundary conditions.

Boundary	Comment	Type	Base value
Convectors			
East convector		Air inlet	$T_{Econvector} = 45\text{ °C}$ $\dot{m}_{Econvector} = 0.048\text{ kg s}^{-1}$
West convector		Air inlet	$T_{Wconvector} = 45\text{ °C}$ $\dot{m}_{Wconvector} = 0.048\text{ kg s}^{-1}$
Walls			
Ceiling		Constant temperature	$T_{ceiling} = 23.2\text{ °C}$
Floor		Constant temperature	$T_{floor} = 18\text{ °C}$
East wall		Constant temperature	$T_{Ewall} = 20\text{ °C}$
West wall		Constant temperature	$T_{Wwall} = 20\text{ °C}$
Windows			
East window	Closed	Air inlet	$T_{Ewindow} = 9.35\text{ °C}$ $\dot{m}_{Ewindow} = 0\text{ kg s}^{-1}$
West window	Closed	Air inlet	$T_{Wwindow} = 8.3\text{ °C}$ $\dot{m}_{Wwindow} = 0\text{ kg s}^{-1}$
Other openings			
East vent		Opening	$T_{Event} = 20.2\text{ °C}$ $P_{Event} = 1.013 \times 10^5\text{ Pa}$
West vent		Opening	$T_{Wvent} = 20.7\text{ °C}$ $P_{Wvent} = 1.013 \times 10^5\text{ Pa}$
Door	Closed		$\dot{m}_{door} = 0\text{ kg s}^{-1}$

2.2. Zone generation

As stated previously, ROMs are created by clustering computational cells of the CFD domain, together depending on their position and their zone criterion. Zone criteria include any variable for which clustering is demanded, including for example temperature, density and air velocity. The method currently uses one criterion at a time, and the ROMs presented in this study have been generated with cell temperature as the zone criterion.

Firstly, zone-types are defined. A zone-type is a group of cells associated with a particular zone criterion over a specific interval, for example, temperatures. Such intervals are defined as follows: first the mean value of the temperature is processed over the entire CFD domain. Two zone-types are then defined: a zone-type containing all the cells in which temperature is higher than the mean value, and another containing all the cells in which temperature is lower or equal to the mean value. Subsequently the zone-types are iteratively subdivided into smaller zone-types, according to the mean value of temperature within each zone-type.

As a result, 2^n zone-types are defined, with n the number of times this process is repeated. The user has control over the number of zone-types as this affects the discretization process. More zone-types allow a higher fidelity to the original CFD, but higher computational costs incur as discussed in the Results section.

Once zone-types have been defined for the ROM, the algorithm starts assigning cells to zones as shown in Fig. 3. A zone is a cluster of computational cells which (1) are adjacent and (2) belong to the same zone-type. The algorithm starts by creating an empty zone and populates it with the first computational cell it finds.

The cells adjacent to this initial cell are scanned, and if they belong to the same zone-type they are added to the zone. The same process is repeated for all the cells in the same zone, until no more

suitable cells are found. At that point the algorithm creates a new zone and repeats the process until all the cells of the domain are assigned to a zone. A previous study [30] by the authors assessed the accuracy of various zone generation algorithms.

Computationally, at this point the original CFD domain has been discretized from the original large number of cells to the final reduced number of zones. Each zone is lumped into a node of the fluid network representing the domain. In order to generate a ROM, it is then necessary to process interactions between fluid nodes, and between fluid nodes and boundary nodes.

2.3. ROM generation

The first step in the ROM generation is to consider zones as uniform volumes in the CFD domain. The average values of temperature, density, and pressure are computed over the cells belonging to each zone in order to obtain the uniform zone properties.

Next, the zone-zone interactions must be computed. The algorithm calculates the mass flow rates at the zone-zone interfaces by selecting all cells that have a neighbour assigned to a different zone and computing the unitary mass flow rate at the interface between these two neighbouring cells. The total mass flow rate between zones is calculated as the sum of all the unitary mass flow rates at the zone-zone interface.

After computing the zone-zone interactions, the algorithm detects the sources of energy such as air inlets and non-adiabatic walls. In a similar fashion to zone-zone interactions, the mass flow rates of inlets/outlets into/from each zone are computed at their interface and the total mass flow rate between an inlet/outlet and a zone is the sum of all unitary mass flow rates. Finally, the thermal boundaries such as non-adiabatic walls are assumed uniform, they are assigned an average temperature and a constant UA depending on their contact area with each zone.

2.4. ROM solution

The ROMs are solved with Sinda/FLUJINT [31], a commercial software for finite-difference lumped parameter fluid flow analysis of complex systems. The data generated from zone properties and interactions with the domain are compiled to respect Sinda/FLUJINT's input format: (1) zones are translated into "tanks", which are lumps of constant volume and uniform properties (temperature, density, pressure); (2) inlets and outlets are translated into "plena", which are similar lumps but with infinite volume; and (3) walls and other purely thermal sources are each translated to a thermal node, with uniform temperature. A thermal and fluid network is then created, linking these elements through corresponding interactions: mass exchange between fluid lumps, and heat exchange between fluid lumps and thermal nodes. Mass exchanges are computed directly from the mass flow rates at zone-zone interfaces found previously, and heat exchanges are computed from a constant UA defined between each zone and thermal boundary. Once the model is solved, Sinda/FLUJINT returns the steady-state solution with properties for each lump which can then be mapped back to the original CFD domain for comparison.

2.5. Error measurement

The present study uses the weighted mean absolute error (WMAE) in units of Kelvin, shown in Equation (1). The weighting corresponds to the volume of each cell relative to the total volume of the domain, in order to account for non-uniform cell volumes, especially close to the boundaries where the CFD mesh is finer.

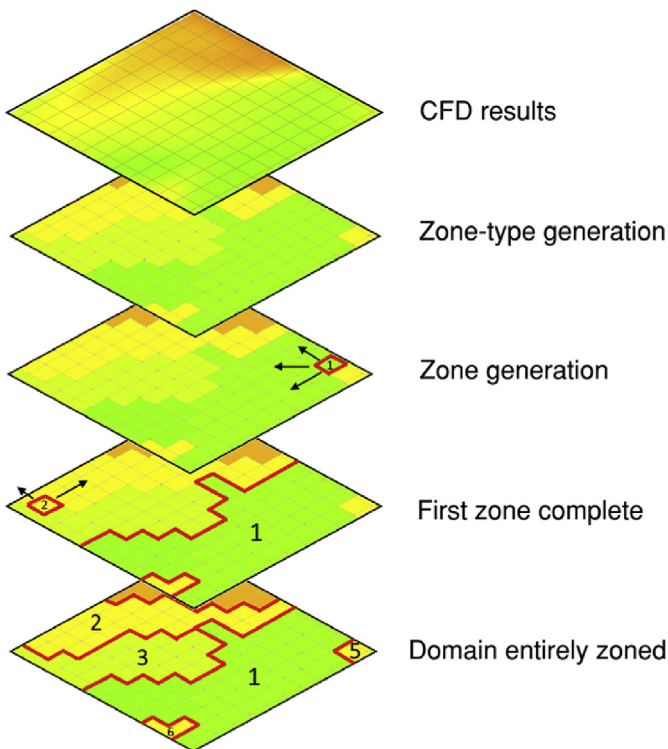


Fig. 3. Representation of the zone generation algorithm in 2 dimensions. The algorithm first defines zone-types and then assigns all adjacent cells of the same zone-type to a new zone.

$$WMAE = \sum_{i=0}^n \frac{V_i \times |T_{CFDi} - T_i|}{V_{domain}} \quad (1)$$

where n is the number of cells in the domain, V_i is the volume of cell i , V_{domain} is the total volume of the domain, T_{CFDi} is the original CFD temperature of cell i , and T_i is the temperature assigned to the cell after solving the ROM.

3. Results

This study presents the results obtained when modifying the parameters of a ROM to predict temperature distributions for BCs that differ from the ones of the original CFD simulations.

In order to achieve this, a set of CFD simulations was generated. For the same computational domain, simulations were solved featuring different inlet temperatures and mass flow rates. Table 2 presents the sets of parameters for boundary conditions used in this study. The CFD simulations, CFD-ROM program and ROM solver have been run on the same desktop computer (Intel Core i7-4790, 8 GB RAM). The cases range from T-10 to T+15 for temperature, including T+5b where only the temperature of the west convector is modified leaving the east one to 45 °C (the base temperature); and from M-45% to M+100% for mass flow rates at the convectors.

ROMs have been generated for zone numbers ranging from 2 to 51 in order to define at which point the error converges. The error quickly decreases for 2–11 zones then stabilizes around 22 zones and is nearly constant thereafter, as shown in Fig. 4, while the corresponding solution times vary from 0.9 s for 2 zones to 1.1 s for 51 zones, against 6–7 h for the CFD simulation. Therefore, the ROMs presented in this study are in the 20–25 zones range, since while the user can demand a certain number of zones, there are occasionally a limited number of odd zones created to accommodate large temperature gradients in the domain. The error in this case is particularly low because the extracted ROM is solved for the same BCs as the original CFD simulation, and as such it does not represent the intended use for the CFD-ROM method. The following section presents the results in the case of ROMs being solved for a different set of BCs and for which CFD results are not available, as would ideally be the case for the application of the CFD-ROM method.

3.1. ROM accuracy when varying boundary condition parameters

Two ROM case studies were generated to (i) measure the impact that changing the ROM parameters has on ROM accuracy, and (ii) assess the usability envelope of ROMs. The first, called “MultiCFD”,

Table 2
List of boundary conditions parameters used in MultiROM and MultiCFD.

Variable	Cases	Values
Temperature ($T_{convector}$)	T-10	35 °C
	T-5	40 °C
	Base	45 °C
	T+5b	50 °C (West) & 45 °C (East)
	T+5	50 °C
	T+10	55 °C
	T+15	60 °C
Mass flow rates ($\dot{m}_{convector}$)	M-45%	0.0528 kg s ⁻¹
	M-30%	0.0672 kg s ⁻¹
	Base	0.096 kg s ⁻¹
	M+30%	0.1248 kg s ⁻¹
	M+45%	0.1392 kg s ⁻¹
	M+60%	0.1536 kg s ⁻¹
	M+100%	0.192 kg s ⁻¹

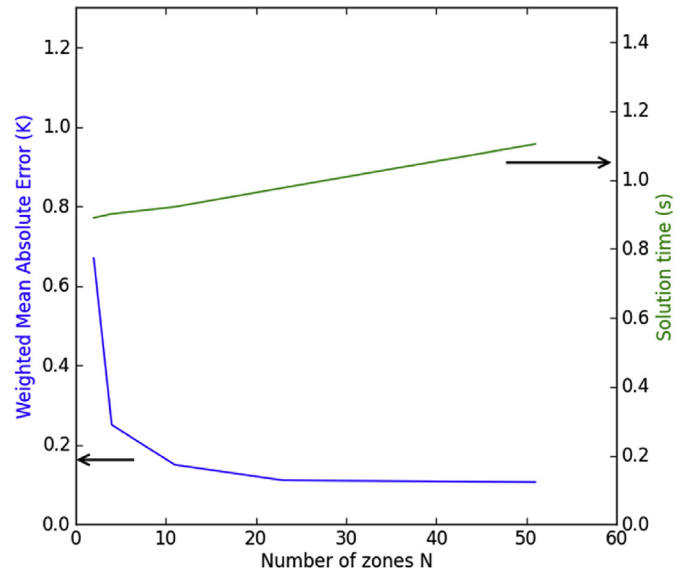


Fig. 4. ROM size independence study.

uses a ROM generated directly from the corresponding CFD case. It serves as a basis for estimating the relative accuracy of the second case study, called “MultiROM”, in which a ROM is generated from the base CFD case and subsequently solved with the new BC parameters. Developing a method for generating flexible and accurate MultiROMs is the main objective of this research. The aim is to provide designers and operators with a tool that would allow them to simulate the built environment when multiple CFD simulations are either unavailable or impractical.

The modelled office and its corresponding CFD simulation feature two convectors for which a temperature and air velocity are defined. This study assesses the accuracy of ROMs when (1) the convectors temperature $T_{convector}$, and (2) their mass flow rate $\dot{m}_{convector}$ are changed. The ROMs are extracted from the “base” CFD case, then their parameters are changed to match the other CFD cases, the ROMs are solved and finally their outputs are compared to the corresponding CFD case results.

The first test was to replicate previous results by the authors

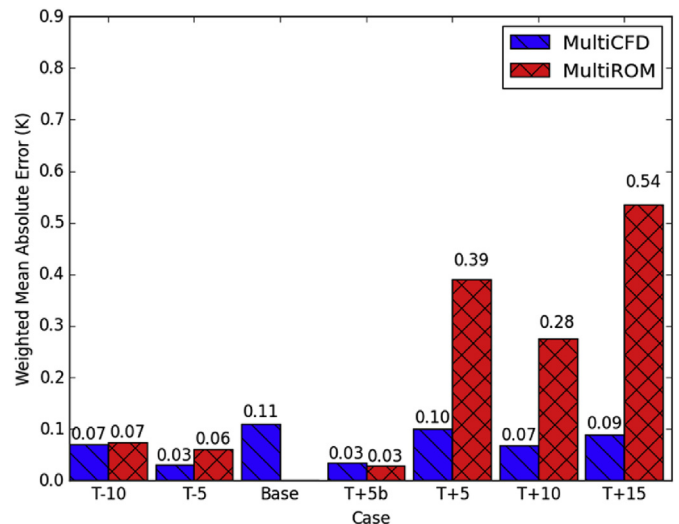


Fig. 5. MultiCFD and MultiROM error when changing BC temperatures.

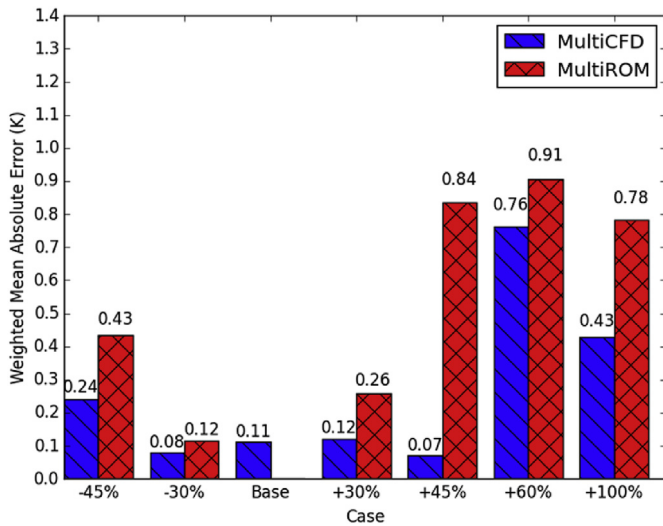


Fig. 6. MultiCFD and MultiROM error when changing BC mass flow rates.

obtained when varying only temperatures by $\pm 5\text{K}$ around the base temperature, then to reach $+15\text{K}$ of variation around the base temperature. Fig. 5 shows the absolute error for each case, in both MultiCFD and MultiROM scenarios. The ROMs show a good level of accuracy when solved for this range of parameters, considering the $\pm 0.6\text{K}$ uncertainty range of temperature sensors commonly met in the built environment [32]. When the temperature is increased above the base temperature, the error is generally higher than ROMs solved for a temperature below the base temperature. This is a result of the immutability of the ROM's zones once they have been generated for the base case. The algorithm generates a fixed

number of zones that cannot be changed after generation. In order to capture certain features, such as large temperature gradients, the algorithm will generate more zones around each feature. In the case of large temperature gradients, the number of zones depends on the amplitude of the gradient: the greater the gradient, the more zones are created. After generation of a ROM from the base case, when it is solved for lower temperatures the gradient is lower and the ROM therefore contains an excess of zones (from the base case) to characterize the smaller gradient, resulting in a smaller error. Conversely, when the ROM is solved for higher temperatures the pre-existing number of zones is not sufficient to capture the larger temperature gradient, resulting in a larger error.

The second, and novel, set of results was generated by varying the convectors mass flow rates. In order to achieve this, an additional function was added to the code to ensure that the ROM mass flow rates were all balanced, as changing the inlets mass flow rates would alter the balance. This step is done in a purely mathematical manner, where zone by zone the inflows and outflows are iteratively balanced to match the new BCs. A connectivity table is generated by comparing the proportion of inflows and outflows from and to each zone and assigning weights to each, so that the general trend of mass exchange in the domain is respected in the modified ROM. The results are presented in Fig. 6 and show that up to $\pm 45\%$ of change in mass flow rates at the convectors, the ROM still has an absolute error under 0.5K versus 0.11K of error for the base, unmodified case – with the exception of the $+45\%$ case with 0.84K of absolute error. This again falls into the uncertainty range of common temperature sensors.

A similar trend exists of higher error for an increase in mass flow rates compared to a lower error for decreased mass flow rates when solving the ROM. This again is due to the immutability of zones once they have been generated, which cannot accommodate a change in flow shape.

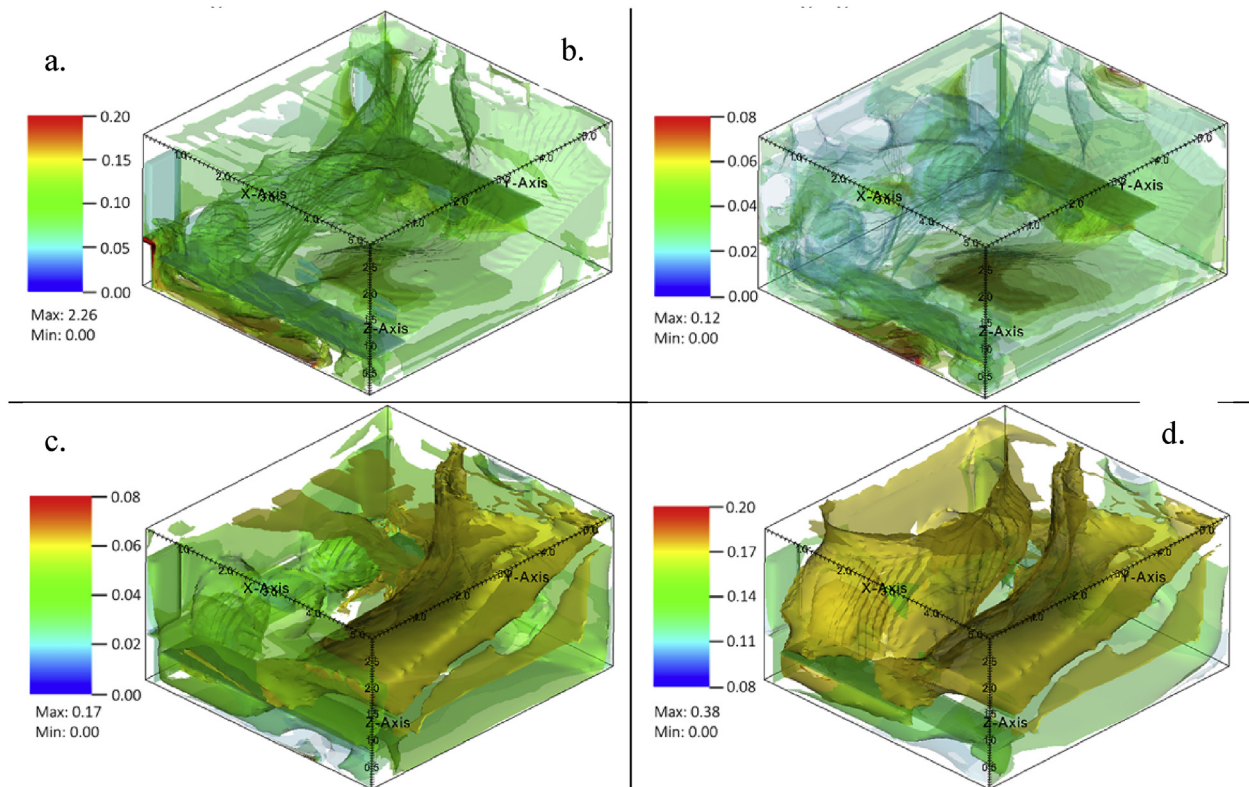


Fig. 7. Iso-surface WMAE (in K) plots of cases (a) $\dot{m}-45\%$, (b) $\dot{m}-30\%$, (c) $\dot{m}+30\%$ and (d) $\dot{m}+45\%$.

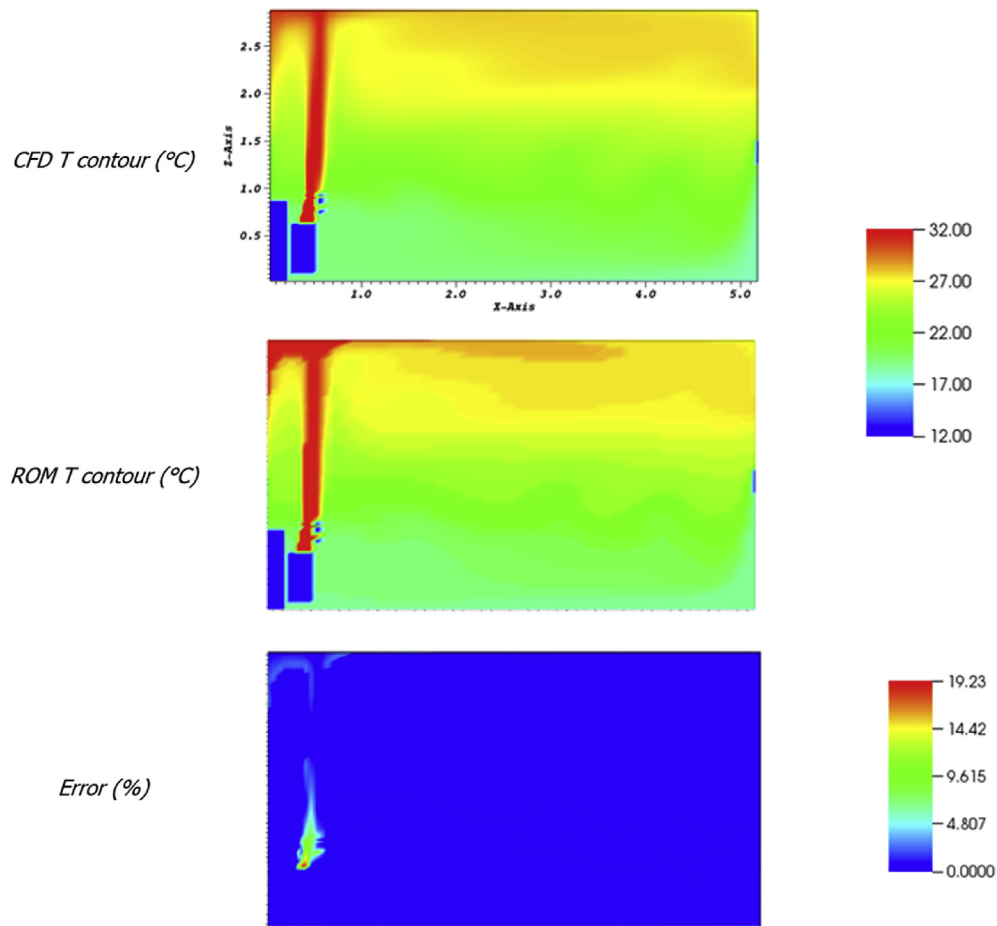


Fig. 8. CFD temperature contour, ROM solution, and error plot of a X–Y slice at the centre of the west convector.

3.2. Error plots

A study of the local error was done in order to assess more finely the fidelity of the ROMs against the original CFD simulations. Fig. 7 shows semi-opaque iso-surface plots of the $\bar{m}-45\%$ to $\bar{m}+45\%$ cases. No peaks in local error stand out, except for a very limited number of odd cells due to minor computational errors. Such errors are due to a mechanism that prevents the algorithm from generating very small zones, which is necessary to avoid assigning too many zones to areas with large temperature gradients. These small zones would not be representative of the flow pattern, but their presence lowers the overall accuracy of the ROM as less zones are available for zoning the remainder of the domain. Without this mechanism, the ROMs would be able to capture large temperature gradients very finely but would be unable to capture stratification.

Results are identical for the T-10 to T+15 cases, suggesting that the algorithm is able to accurately capture the domain's thermal distribution, including the volumes with high temperature gradients such as above and around the convectors. Fig. 8 shows a X-Z slice of the domain at the centre of the west convector and shows how the CFD-ROM method captures both the heat plume above the convector and also temperature stratification in the room. The limited error visible around the heat plume shows that setting a lower limit to the size of zones does not adversely affect to a great extent the algorithm's ability to capture high temperature gradients, while allowing it to also capture smaller variations in temperature.

4. Discussion

This study showed that it is possible to extract multi-zonal ROMs from CFD simulations with high fidelity and in real time for application domains in the built environment. These findings can be mitigated by the relative simplicity of the case study utilised in this research, where only two convectors and two vents are present in the domain. Further research must be done on other indoor environments, such as open-space offices, theatre rooms or sports complexes in order to assess the usability of the method in more complex environments featuring larger spaces and openings, air vents, HVAC outlets, which could affect the accuracy of the ROMs.

Furthermore, it is currently up to the end user to select an appropriate number of zones for the ROM. An extreme example would be the selection of a 20-zone ROM in a domain with 19 air inlets: the algorithm would use 19 of the available zones to capture the air inlets, and only one to capture the rest of the domain. In order to generate a more appropriate number of zones it might be beneficial to set an upper limit to the size of each zone, so that the algorithm could if needed increase the number of zones without user input. There is a certain room for expansion in the number of zones, as this study has shown that the difference in time to solution between 3 and 50 zones is not significant and 20–25 zones are enough to model the presented case, yet further research must be done on complex scenarios to certify the usability of this method for larger numbers of zones.

In both studies, when varying temperature and mass flow rates

the ROMs are generally more accurate when lowering the parameters values than they are when the values are increased. When solving for different BCs, the parameters computed on the base case are not valid anymore and lead to increasing error as the new ROM differs more and more from the base case. This is likely caused by the immutability of zones after they have been generated from the base case and the assumptions made when compiling the model for Sinda/FLUJINT, namely the constant values assigned to zone-zone mass flow rates and wall heat transfers. An improvement upon the current iteration of the method will be the implementation of variable mass flow rates and heat transfers. The asymmetrical change in error, lower when temperatures are colder and mass flow rates weaker, is due to the fact that the domain becomes more and more uniform as the energy flow in the domain is lower, in which case the ROM has more zones than necessary to compute the new temperature distributions. Increasing the number of zones globally lowers the error but the asymmetry is still present to some extent.

Nevertheless, the results are encouraging when considering the usual $\pm 0.6\text{K}$ uncertainty of temperature sensing techniques in the built environment [32]. The possibility to change boundary temperatures by $\pm 15\text{K}$ and mass flow rates by $\pm 45\%$ while maintaining an acceptable level of accuracy allows the consideration of, for example, thermal comfort and HVAC control as potential applications for which further research must be done.

Additionally, the authors consider the inclusion of multiple-criteria zone generation, versus the current single-criterion zone generation, as an important upgrade to the algorithm which may improve its accuracy especially when mass flow rates must be changed.

5. Conclusion

The accuracy of CFD is recognized to have a potentially substantial impact on building energy consumption through methods such as virtual sensing [33]. Unfortunately, the computational costs involved in solving a CFD model render it unpractical for real-time applications such as BEMS. This study proposed a method capable of extracting ROMs from CFD simulations and solving them in near real-time. First an ROM size independence study was conducted, showing that it can be achieved for 20 to 25 zones for the presented case. The accuracy of ROMs that were solved and assessed for (1) different temperature BCs and (2) different mass flow rates. It was shown that it was possible to obtain accurate results, in real time, for boundary conditions that were different from the original CFD BCs. These multi-zonal ROMs have an accuracy comparable to the uncertainty in sensing equipment used in the built environment, thus rendering them useful in applications such as virtual sensing. This enables the use of CFD-ROM for thermal comfort assessment, BEMS, and applications where the unavailability of real-time zonal models is detrimental.

However, it is necessary to apply this method to more complex scenarios in order to confirm its advantages in terms of rapidity and accuracy, and it is also necessary to include additional features such as multi-criteria zone generation and a radiation model. Currently the authors are studying CFD simulations of a highly glazed, naturally ventilated room to further improve the CFD-ROM method, and look forward to applying the method to larger, more complex cases.

The next steps in the development of the CFD-ROM toolchain are: (1) the generation of ROMs for different indoor environments, such as highly glazed, naturally ventilated rooms; (2) the investigation of techniques that would improve ROMs accuracy when solving for different inlet mass flow rates; (3) the inclusion of a radiation model; and (4) the development of a tailored solver in the open-source language Modelica [34].

CRedit authorship contribution statement

Thibault Marzullo: Conceptualization, Methodology, Software, Validation, Formal analysis, Investigation, Data curation, Writing - original draft, Visualization. **Marcus M. Keane:** Conceptualization, Resources, Writing - review & editing, Supervision, Project administration, Funding acquisition. **Marco Geron:** Conceptualization, Methodology, Validation, Resources, Writing - review & editing, Supervision. **Rory F.D. Monaghan:** Conceptualization, Methodology, Resources, Writing - review & editing, Supervision, Project administration, Funding acquisition.

Acknowledgements

The authors wish to acknowledge the following funding. T. Marzullo is supported by a Scholarship from the College of Engineering and Informatics at NUI Galway and by HIT2GAP (EU/H2020 Grant Agreement No.: 680708).

References

- [1] Ma W, Fang S, Liu G, Zhou R. Modeling of district load forecasting for distributed energy system. *Appl Energy* Oct. 2017;204:181–205.
- [2] Cai H, Ziras C, You S, Li R, Honoré K, Bindner HW. Demand side management in urban district heating networks. *Appl Energy* Nov. 2018;230:506–18.
- [3] Nageler P, Schweiger G, Schranzhofer H, Mach T, Heimrath R, Hochenauer C. Novel method to simulate large-scale thermal city models. *Energy* Aug. 2018;157:633–46.
- [4] Allegrini J, Orehounig K, Mavromatidis G, Ruesch F, Dorer V, Evins R. A review of modelling approaches and tools for the simulation of district-scale energy systems. *Renew Sustain Energy Rev* Dec. 2015;52:1391–404.
- [5] Fraisse G, Viardot C, Lafabrie O, Achard G. Development of a simplified and accurate building model based on electrical analogy. *Energy Build* 2002;34(10):1017–31.
- [6] Hillary J, Walsh E, Shah A, Zhou R, Walsh P. Guidelines for developing efficient thermal conduction and storage models within building energy simulations. *Energy* Apr. 2017;125:211–22.
- [7] Harish VSKV, Kumar A. Reduced order modeling and parameter identification of a building energy system model through an optimization routine. *Appl Energy* 2016;162:1010–23.
- [8] Shaikh PH, Nor NBM, Nallagownden P, Elamvazuthi I, Ibrahim T. A review on optimized control systems for building energy and comfort management of smart sustainable buildings. *Renew Sustain Energy Rev* 2014;34:409–29.
- [9] Megri AC, Haghighat F. Zonal modeling for simulating indoor environment of buildings: review, recent developments, and applications. *HVAC R Res* 2007;13(6):887–905.
- [10] Blocken B, Tominaga Y, Stathopoulos T. CFD simulation of micro-scale pollutant dispersion in the built environment. *Build Environ* Jun. 2013;64:225–30.
- [11] Zhao X, Liu W, Lai D, Chen Q. Optimal design of an indoor environment by the CFD-based adjoint method with area-constrained topology and cluster analysis. *Build Environ* Jun. 2018;138:171–80.
- [12] van Hooff T, Blocken B. CFD evaluation of natural ventilation of indoor environments by the concentration decay method: CO₂ gas dispersion from a semi-enclosed stadium. *Build Environ* Mar. 2013;61:1–17.
- [13] Etheridge D. A perspective on fifty years of natural ventilation research. *Build Environ* Sep. 2015;91:51–60.
- [14] Mochida A, Lun IYF. Prediction of wind environment and thermal comfort at pedestrian level in urban area. *J Wind Eng Ind Aerodyn* Oct. 2008;96(10–11):1498–527.
- [15] Moonen P, Dorer V, Carmeliet J. Evaluation of the ventilation potential of courtyards and urban street canyons using RANS and LES. *J Wind Eng Ind Aerodyn* Apr. 2011;99(4):414–23.
- [16] Blocken B, Persoon J. Pedestrian wind comfort around a large football stadium in an urban environment: CFD simulation, validation and application of the new Dutch wind nuisance standard. *J Wind Eng Ind Aerodyn* Aug. 2009;97(5–6):255–70.
- [17] Hang J, Li Y, Sandberg M, Buccolieri R, Di Sabatino S. The influence of building height variability on pollutant dispersion and pedestrian ventilation in idealized high-rise urban areas. *Build Environ* Oct. 2012;56:346–60.
- [18] Buccolieri R, Sandberg M, Di Sabatino S. City breathability and its link to pollutant concentration distribution within urban-like geometries. *Atmos Environ* May 2010;44(15):1894–903.
- [19] Gromke C, Buccolieri R, Di Sabatino S, Ruck B. "Dispersion study in a street canyon with tree planting by means of wind tunnel and numerical investigations – evaluation of CFD data with experimental data. *Atmos Environ* Dec. 2008;42(37):8640–50.
- [20] Issa RI. Solution of the implicitly discretised fluid flow equations by operator-

- splitting. *J Comput Phys* 1986;62(1):40–65.
- [21] Patankar S, Spalding D. A calculation procedure for heat, mass and momentum transfer in three-dimensional parabolic flows. *Int J Heat Mass Transf* Oct. 1972;15(10):1787–806.
- [22] Xue Y, Liu W, John Zhai Z. New semi-Lagrangian-based PISO method for fast and accurate indoor environment modeling. *Build Environ* 2016;105:236–44.
- [23] Bakewell HP. Viscous sublayer and adjacent wall region in turbulent pipe flow. *Phys Fluids* 1967;10(9):1880.
- [24] Willcox KE, Peraire J. Balanced model reduction via the proper orthogonal decomposition. *AIAA J* 2002;40(11):2323–30. SRC-GoogleScholar FG-0.
- [25] Robert A. A stable numerical integration scheme for the primitive meteorological equations. *Atmos-Ocean* 1981;19(1):35–46.
- [26] Chorin AJ. A numerical method for solving incompressible viscous flow problems. *J Comput Phys* 1967;2(1):12–26.
- [27] Python Software Foundation., "Python language reference, version 2.7." .
- [28] Mullen DT, Keane MM, Geron M, Monaghan RFD. Automatic extraction of reduced-order models from CFD simulations for building energy modelling. *Energy Build* Jul. 2015;99:313–26.
- [29] Rosten H, Spalding D, Tatchell D. PHOENICS: a general-purpose program for fluid-flow, heat transfer and chemical-reaction processes. *CHAM*; 1983.
- [30] Marzullo T, Yousefian S, Keane MM, Geron M, Monaghan RFD. A comparative study of computational algorithms used in the automatic generation of reduced-order models from CFD simulations. In: In 3rd building simulation Applications conference proceedings; 2017.
- [31] SINDA/FLUINT." [Online]. Available: www.crtech.com/sinda.html. [Accessed: 20-Jul-2016].
- [32] Li H, Yu D, Braun JE. A review of virtual sensing technology and application in building systems. *HVAC R Res* 2011;9669:37–41.
- [33] Tan H, Dexter L. Improving the accuracy of sensors in building automation systems. In: In proceedings of the 16th IFAC world congress; 2005.
- [34] Fritzson P, Engelson V. Modelica-A unified object-oriented language for system modeling and simulation 1998;1445:67–90. ECOOP'98-Object-Oriented Program.